Observations of seasonal upwelling and downwelling in the Beaufort Sea mediated by sea ice

(submitted to J. Phys. Oceanogr.)

GIANLUCA MENEGHELLO, JOHN MARSHALL,
MARY-LOUISE TIMMERMANS, JEFFERY SCOTT

Key points

- **Ten years mean Ekman downwelling is only 2.5 $m/year$.**
- **Strong autumn downwelling is partially compensated by winter upwelling driven by the geostrophic current below fast ice.**
- **Important regional patterns of upwelling and downwelling are identified.**

Method

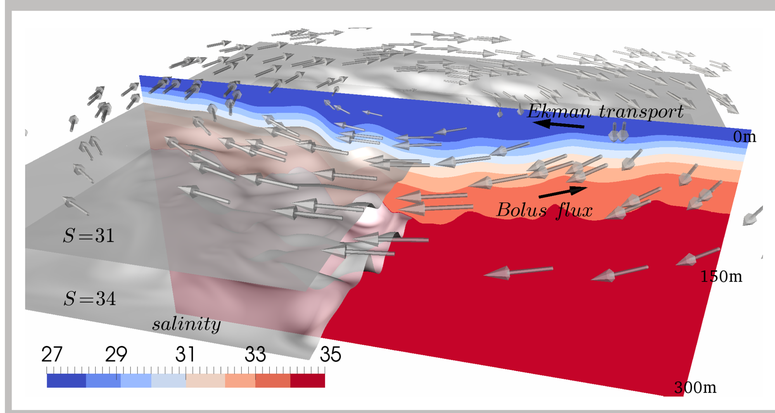

We compute the surface-ocean stress $\boldsymbol{\tau}$ as a combination of ice-ocean and air-ocean surface stresses, each estimated using a quadratic drag law with fixed drag coefficients ($C_{Di} = 0.0055$, $C_{Da} = 0.00125$), and weighted by the observed local ice concentration α (Yang, 2006, 2009):

$$\boldsymbol{\tau} = \alpha \underbrace{\rho C_{Di} \left|\boldsymbol{u}_{rel}\right| \left(\boldsymbol{u}_{rel}\right)}_{\boldsymbol{\tau}_i} + (1-\alpha) \underbrace{\rho_a C_{Da} \left|\boldsymbol{u}_a\right| \left(\boldsymbol{u}_a\right)}_{\boldsymbol{\tau}_a},$$

where the ice-ocean relative velocity $\boldsymbol{u}_{rel}$ may be written in terms of the ice velocity $\boldsymbol{u}_i$, the surface geostrophic velocity $\boldsymbol{u}_g$, and the Ekman velocity $\boldsymbol{u}_e$ as $\boldsymbol{u}_{rel} = \boldsymbol{u}_i - (\boldsymbol{u}_g + \boldsymbol{u}_e)$. The Ekman pumping rate is then computed making use of the daily stress fields as

$$w_{Ek} = \nabla \times \boldsymbol{\tau}/(\rho f).$$

Climatology

Four datasets are combined to estimate the surface ocean stress $\boldsymbol{\tau}$ and Ekman pumping w_{Ek}: (i) sea ice concentration α from Nimbus-7 SMMR and DMSP SSM/I-SSMIS Passive Microwave Data Version 1 (Cavalieri et al., 1996); (ii) sea ice velocity $\boldsymbol{u}_i$ from the Polar Pathfinder Daily 25 km EASE-Grid Sea Ice Motion Vectors, Version 3 (Tschudi et al., 2016); (iii) geostrophic currents $\boldsymbol{u}_g$ computed from Dynamic Ocean Topography (Armitage et al., 2016, 2017) and (iv) 10 m wind $\boldsymbol{u}_a$ from the NCEP-NCAR Reanalysis 1 (Kalnay et al., 1996). The four different datasets, defined on different grids, are interpolated on a common EASE-25 km polar stereographic equal area grid, which is the native grid for the ice velocity.

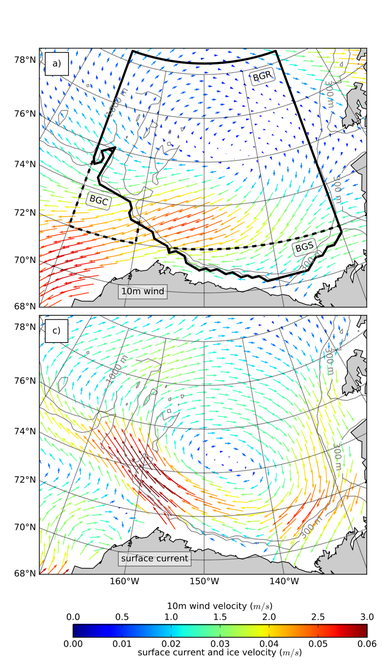

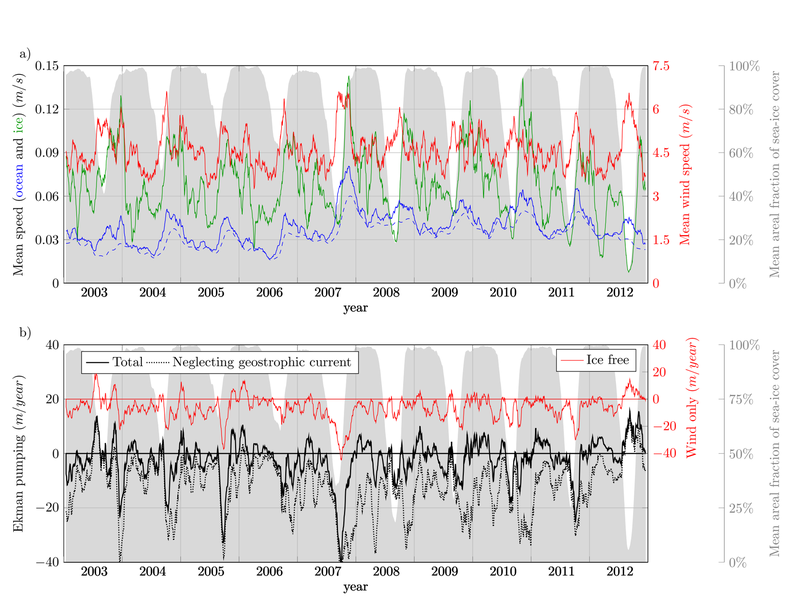

Ten year means (2003-2012) of: a) 10 m wind, b) ice velocity, c) surface geostrophic current and d) ice edge (15% ice concentration) for August, September, and October (the ice concentration is larger than 15% everywhere for the rest of the year). The thick black line delimits the Beaufort Gyre Region (BGR); while dashed lines delimit the Beufort Gyre Chukchi Sea in the south-west (BGC) and the Beaufort Gyre Southern regions of the BGR (BGS).

(a) Thirty-day running mean of 10 m wind velocity $\boldsymbol{u}_a$ (red), ice velocity $\boldsymbol{u}_i$ (green), surface geostrophic current velocity $\boldsymbol{u}_g$ (dashed blue), surface ocean velocity $\boldsymbol{u}_g + \boldsymbol{u}_e$ (solid blue), and sea ice concentration α.
(b) Thirty-day running mean Ekman pumping (solid black), Ekman pumping in the absence of geostrophic current (dotted black) and Ekman pumping for a completely ice free BGR (red, note axes on the right). Gray areas in both panels show ice concentration.

Effect of the geostrophic current

To better understand the relative role of the winds, sea-ice and ocean geostrophic currents, we additionally compute the contribution of the geostrophic current to the ice stress as

$$\boldsymbol{\tau}_{ig} = \boldsymbol{\tau}_i - \boldsymbol{\tau}_{i0}$$

where $\boldsymbol{\tau}_{i0}$ is the ice-ocean stress neglecting the geostrophic current, i.e., computed by setting $\boldsymbol{u}_g = 0$.

BEAUFORT GYRE REGION (BGR)

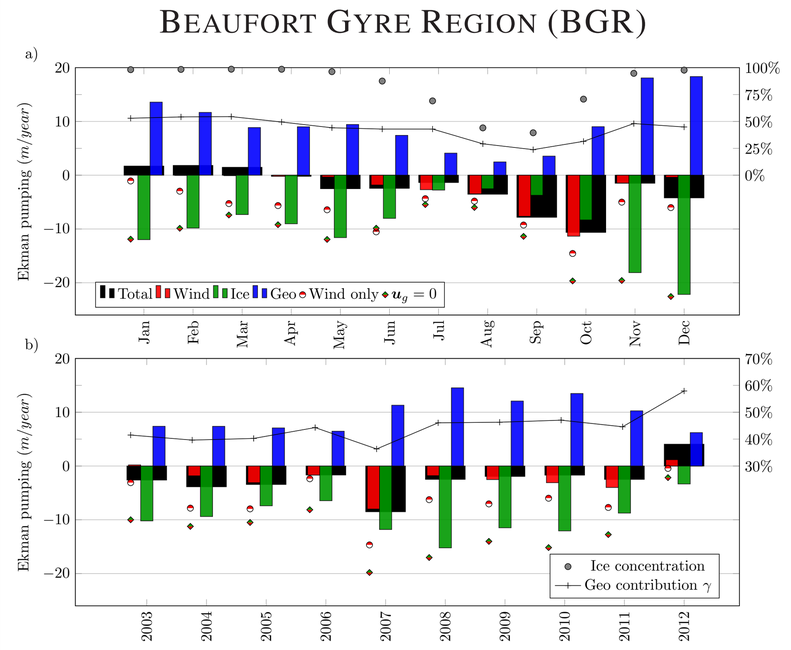

CHUKCHI SEA REGION (BGC)

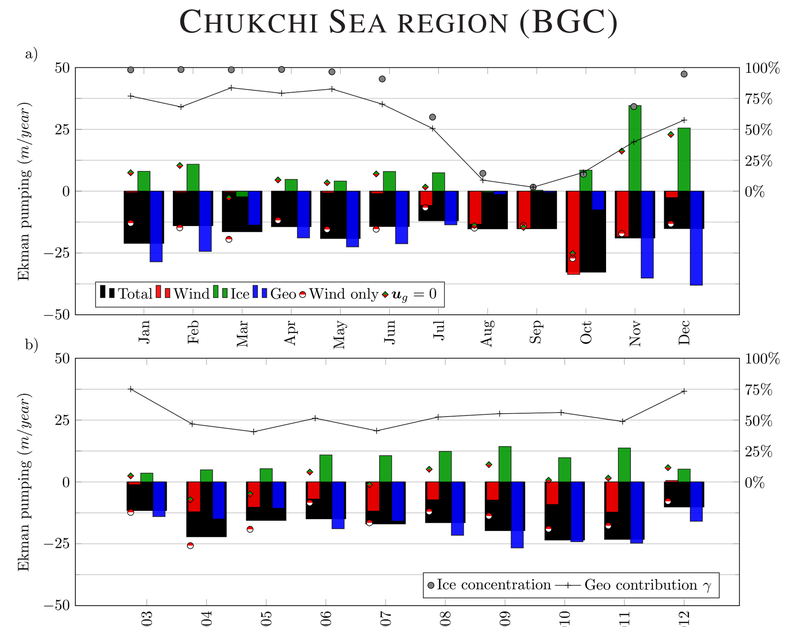

Area averaged monthly (a) and yearly (b) values of Ekman pumping (black bars) and its three main components: w_a (red bars, pumping over the open ocean), w_{i0} (green bars, pumping in the ice-covered ocean in the absence of a geostrophic current) and w_{ig} (blue bars, modification of under-ice pumping due to ocean currents). The red and green diamonds give the total Ekman pumping $w_a + w_{i0}$ in the absence of an ocean geostrophic contribution. The red and white circles give the wind driven Ekman pumping w_A in a completely ice free BGR. The pumping scale is on the left. The thin black line is a measure of the importance of geostrophic currents γ (scale on the right hand side). The gray circles in the top panel (a) indicate the ice concentration α (scale on the right).

$$w_a = \frac{\nabla \times ((1-\alpha)\boldsymbol{\tau}_a)}{\rho f} \qquad w_i = \frac{\nabla \times (\alpha \boldsymbol{\tau}_i)}{\rho f}$$

$$w_{i0} = \frac{\nabla \times (\alpha \boldsymbol{\tau}_{i0})}{\rho f} \qquad w_{ig} = \frac{\nabla \times (\alpha \boldsymbol{\tau}_{ig})}{\rho f}$$

$$w_A = \frac{\nabla \times \boldsymbol{\tau}_a}{\rho f} \qquad \gamma = \frac{|w_{ig}|}{|w_a| + |w_{i0}| + |w_{ig}|}$$

Climatology — Ekman pumping Maps

Monthly Climatology

Yearly Climatology

Climatology of Ekman pumping field in $m/year$. The black dashed lines denotes the limits of the BGR, BGS and BGC regions. Gray thick lines mark the location where the geostrophic current component contribution is zero. Interior to this line, the geostrophic current gives an upwelling contribution, outside (e.g., towards the coast in the south) it enhances downwelling.

References

Armitage, T. W. K., Bacon, S., Ridout, A. L., Petty, A. A., Wolbach, S., and Tsamados, M. (2017). Arctic Ocean geostrophic circulation 2003-2014. *The Cryosphere Discussions*, 2017:1–32.

Armitage, T. W. K., Bacon, S., Ridout, A. L., Thomas, S. F., Aksenov, Y., and Wingham, D. J. (2016). Arctic sea surface height variability and change from satellite radar altimetry and GRACE, 2003-2014. *Journal of Geophysical Research: Oceans*, 121(6):4303–4322.

Cavalieri, D. J., Parkinson, C. L., Gloersen, P., and Zwally, H. J. (1996). Sea Ice Concentrations from Nimbus-7 SMMR and DMSP SSM/I-SSMIS Passive Microwave Data, Version 1.

Kalnay, E., Kanamitsu, M., Kistler, R., Collins, W., Deaven, D., Gandin, L., Iredell, M., Saha, S., White, G., Woollen, J., Zhu, Y., Chelliah, M., Ebisuzaki, W., Higgins, W., Janowiak, J., Mo, K. C., Ropelewski, C., Wang, J., Leetmaa, A., Reynolds, R., Jenne, R., and Joseph, D. (1996). The NCEP/NCAR 40-year reanalysis project. *Bulletin of the American Meteorological Society*, 77(3):437–471.

Tschudi, M., Fowler, C., Maslanik, J. S., and Meier, W. (2016). Polar Pathfinder Daily 25 km EASE-Grid Sea Ice Motion Vectors, Version 3.

Yang, J. (2006). The seasonal variability of the Arctic Ocean Ekman transport and its role in the mixed layer heat and salt fluxes. *Journal of Climate*, 19(20):5366–5387.

Yang, J. (2009). Seasonal and interannual variability of downwelling in the Beaufort Sea. *J Geophys Res*, 114:C00A14.